

Holography with incoherent light

Akanksha Gautam ¹, Athira TS ², Dinesh N. Naik ², C.S. Narayanmurthy ², Rajeev Singh ¹ and Rakesh Kumar Singh ^{1,*}

¹ Laboratory of Information Photonics and Optical Metrology, Department of Physics, Indian Institute of Technology, (Banaras Hindu University), Varanasi, Uttar Pradesh, India; krakeshsingh.phy@iitbhu.ac.in

² Applied and Adaptive Optics Laboratory, Department of Physics, Indian Institute of Space Science and Technology, Thiruvananthapuram-695547, India; dineshnaik@iist.ac.in

* Correspondence: akankshagautam1007@gmail.com

Abstract: Conventional digital holography uses the technique of combining two coherent light fields and the numerical reconstruction of the recorded hologram leads to the object amplitude and phase information. In spite of significant developments on the DH with coherent light, complex field imaging with arbitrary coherent source is also desired for various reasons. Here, we present a possible experimental approach for holography with the incoherent light. In case of incoherent light, the complex spatial coherence function is a measurable quantity and the incoherent object holograms are recorded as the coherence function. Thus, to record complex spatial coherence a square Sagnac radial shearing interferometer is designed with the phase-shifting approach. The five-step phase-shifting method helps to measure the fringe visibility and the corresponding phase, which jointly represents the complex coherence function. The inverse Fourier transform of complex coherence function helps to retrieve the object information.

Keywords: Digital holography; Interference; Coherence; Phase-shifting

1. Introduction

Digital holography (DH) is a technique of interference of two waves both spatially and temporally coherent [1]. The recorded interference pattern contains both amplitude and phase information which can be further reconstructed on digitally processing of the recorded hologram [2, 3]. The coherent source is utilized to achieve the interference in the DH, but the coherent imaging system suffers from speckle noise and edge effects [4, 5]. Whereas, the incoherent imaging systems both spatially and temporally incoherent, such as broad band or a light emitting diode (LED) do not suffer from speckle noise and also cost effective. Therefore, over the coherent imaging systems the incoherent imaging systems are preferred for certain applications.

The interference of incoherent light reflected or emitted from an object result in incoherent digital holograms. Many known methods of recording incoherent holograms are based on the self-interference principle which uses the property that each incoherent source point is acting as an independent scatterer and is self-spatially coherent and hence, it can generate an interference pattern with light coming from its mirror imaged point [6–8]. These techniques record the incoherent hologram in the form of intensity patterns. The other way to record an incoherent hologram is in the form of two-point spatial complex coherence function [9, 10]. These methods are based on the van Cittert-Zernike (VCZ) theorem which connects the far-field complex coherence function with the incoherent source intensity distribution.

In this paper, we present an experimental approach to record an incoherent object hologram based on the VCZ theorem and present some initial results. In the first part of the set up the object information is recorded as a two-point complex spatial coherence function and in the later part a square Sagnac radial shearing interferometer with five-step phase-shifting technique is designed to obtain the complex coherence function. The digital inverse Fourier transform of complex coherence function helps to retrieve the object information.

2. Principle

The principle of coherence holography is based on the existing similarity between the VCZ theorem and the diffraction integral. The VCZ theorem connects the coherence function of the incoherent source with its intensity distribution through the Fourier transform relation. Consider a resolution target (number '5') incoherently illuminated by a yellow LED having spectral scattering density $\eta(\tilde{\mathbf{r}}; \lambda)$ where λ is the mean wavelength of the LED and $\tilde{\mathbf{r}}$ is the transverse coordinate, respectively. As the source is incoherent each point of LED is acting as random scatterer having instantaneous phase $\phi(\tilde{\mathbf{r}}, t)$. The spectral component of the field is given by $A(\tilde{\mathbf{r}}; \lambda) = \sqrt{\eta(\tilde{\mathbf{r}}; \lambda)} \exp[i\phi(\tilde{\mathbf{r}}, t)]$ corresponding to λ . The field is Fourier transformed using a lens L having a focal length f and at Fourier plane, a single realization of the field is represented as

$$E(\mathbf{r}) = \iint A(\tilde{\mathbf{r}}; \lambda) \exp\left(-\frac{i2\pi}{\lambda f}(\mathbf{r} \cdot \tilde{\mathbf{r}})\right) d\tilde{\mathbf{r}} \quad (1)$$

where \mathbf{r} is the coordinate of Fourier plane.

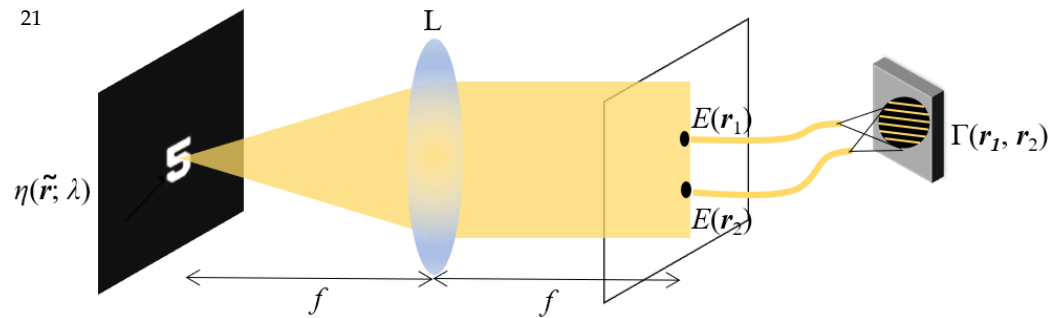


Figure 1. Geometry for recording information of spatial coherence function

The coherence function at the Fourier plane is given by

$$\Gamma(\mathbf{r}_1, \mathbf{r}_2) = \langle E^*(\mathbf{r}_1)E(\mathbf{r}_2) \rangle \quad (2)$$

where the asterisk represents complex conjugate and angle bracket denotes the ensemble average.

From Eq. (1), we can write

$$\Gamma(\mathbf{r}_1, \mathbf{r}_2) = \frac{\kappa}{\lambda^2 f^2} \iint \sqrt{\eta(\tilde{\mathbf{r}}_1; \lambda)\eta(\tilde{\mathbf{r}}_2; \lambda)} \langle \exp[i(\phi(\tilde{\mathbf{r}}_2, t) - \phi(\tilde{\mathbf{r}}_1, t))] \exp\left[-i\frac{2\pi}{\lambda f}(\mathbf{r}_2 \cdot \tilde{\mathbf{r}}_2 - \mathbf{r}_1 \cdot \tilde{\mathbf{r}}_1)\right] d\tilde{\mathbf{r}}_1 d\tilde{\mathbf{r}}_2 \quad (3)$$

where κ is a constant physical quantity having dimensions of length square. As the LED source is spatially incoherent any two points of the source are mutually uncorrelated and hence represented by a two-dimensional (2-D) Dirac-delta function

$$\langle \exp[i(\phi(\tilde{\mathbf{r}}_2, t) - \phi(\tilde{\mathbf{r}}_1, t))] \rangle = \delta(\tilde{\mathbf{r}}_2 - \tilde{\mathbf{r}}_1)$$

The Eq. (3) is now reduced to

$$\Gamma(\mathbf{r}_1, \mathbf{r}_2) = \frac{\kappa}{\lambda^2 f^2} \left\{ \int \eta(\tilde{\mathbf{r}}; \lambda) \exp\left[-i\frac{2\pi}{\lambda f}\tilde{\mathbf{r}} \cdot (\mathbf{r}_2 - \mathbf{r}_1)\right] d\tilde{\mathbf{r}} \right\} d\lambda \quad (4)$$

In the above equation an integration is also performed over the wavelength range λ as the source is non-monochromatic and have a finite spectral bandwidth. The integral inside the curly bracket represents van Cittert-Zernike theorem.

3. Experiment and results

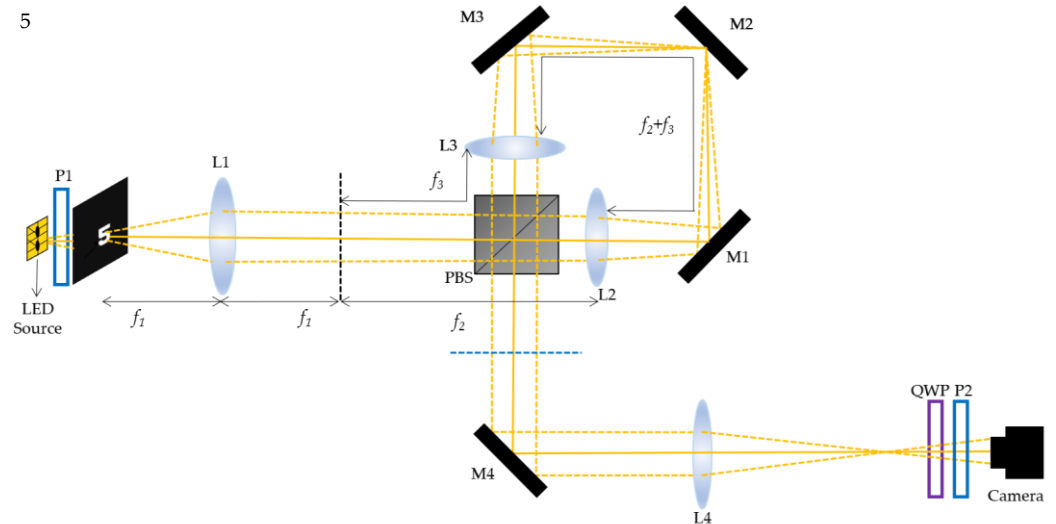


Figure 2. Experimental set up square Sagnac radial shearing interferometer: P: Polarizer, L: Lens, BS: Beam Splitter, M: Mirror, QWP: Quarter Wave Plate

Fig. 2 shows the experimental set up to record the spatial coherence function. The first part of the set up shows the recording of object information as explained in previous section. A polarizer P1 is kept at 45° just after the LED source to make the unpolarized light coming from the LED polarized. The field is Fourier transformed using a lens L1 kept at its focal length $f_1 = 60$ mm from the target, number '5'. The black dotted line shows the Fourier plane where the spatial coherence function represented by Eq. (4) is present. In the later part, a square Sagnac radial shearing interferometer with a telescopic lens system L2 ($f_2 = 120$ mm) and L3 ($f_3 = 125$ mm) is designed to measure the coherence function. The incoming field is divided by a polarizing beam splitter with orthogonal polarization states in two parts and between the two oppositely counter propagating beams one gets magnified with magnification $\alpha = f_3/f_2$ and the other gets demagnified with magnification $\alpha^{-1} = f_2/f_3$. Finally, at the output plane shown by blue dotted lines we get radially sheared copies of the two fields. The output plane parameters are now scaled as $r_1 = \alpha^{-1}r$ and $r_2 = \alpha r$ and the coherence function $\Gamma(r_1, r_2)$ is now mapped as $\Gamma(\alpha^{-1}r, \alpha r)$. The output plane doesn't fit the CMOS camera area (Thorlabs DCC3240M, imaging area 6.78 mm x 5.43 mm with pixel size 5.3 μm) so, an imaging lens L4 with focal length $f_4 = 150$ mm is used to demagnify the image such that it fits the camera aperture. At the output, just before the camera, a quarter wave plate (QWP) is kept at 45° from its fast axis to convert the two linear orthogonal polarization states in right circular and left circular polarization states, respectively. Later, a polarizer P2 is kept and rotated by angle θ such that it introduces a phase shift 2θ between the two incoming beams. Five off-axis interferograms with phase shift $0, \pi/2, \pi, 3\pi/2$ and 2π are recorded by giving a tilt using mirror M2 between the two counter propagating beams. The fringe contrast γ and corresponding phase ϕ' can be calculated as mentioned in references [11] and [12], respectively. Thus, the complex spatial coherence function is built as $\Gamma(\alpha^{-1}r, \alpha r) = \gamma \exp(i\phi')$.

Now, to reconstruct the object intensity distribution the spatial coherence function is inverse Fourier transformed

$$\tilde{\eta}(\tilde{\mathbf{r}}; \lambda) = (\alpha - \alpha^{-1})^2 \int \Gamma(\alpha^{-1}\mathbf{r}, \alpha\mathbf{r}) \exp \left[i \frac{2\pi}{\lambda f} (\alpha - \alpha^{-1}) \mathbf{r} \cdot \tilde{\mathbf{r}} \right] d\mathbf{r} \quad (5)$$

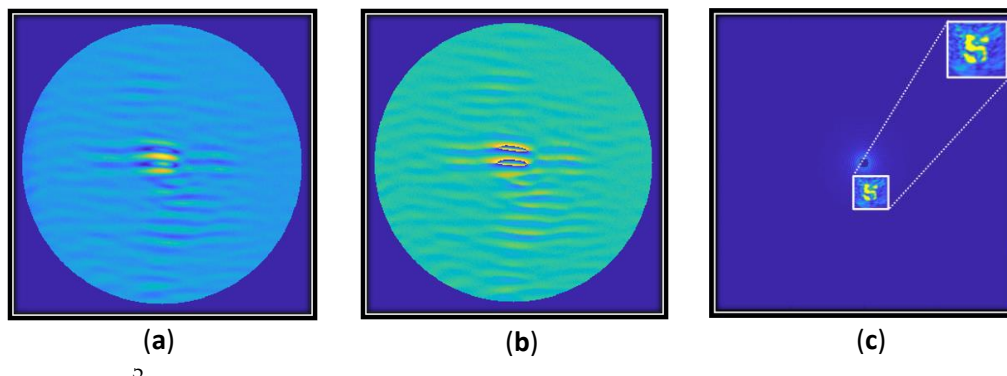


Figure 3. Digitally constructed coherence function (a) fringe visibility (b) corresponding phase and (c) reconstructed object intensity distribution

Fig. 3 represents the digitally constructed (a) fringe visibility and (b) corresponding phase using the five recorded interferograms and (c) the reconstructed object intensity distribution showing the information of number '5'.

4. Conclusion

We have presented an experimental method using shearing for holography with the incoherent source. The object information is recorded in the form of complex spatial coherence function based on the principle of van Cittert-Zernike theorem and later it is analysed using a Sagnac radial shearing interferometer with the five-phase shifting algorithm. The object information is computationally acquired on inverse Fourier transform.

Author Contributions: Akanksha Gautam: Conceived the idea, Investigation, Writing manuscript, Methodology, Experimental Design. Athira TS: Experimental Design. Dinesh N. Naik: Ideas, Revision and editing, Supervision. C.S. Narayanmurthy: Editing and revision of manuscript. Rajeev Singh: Editing and revision of manuscript. Rakesh Kumar Singh: Ideas, Formulation of research goals, Revision and editing, Funding acquisition, Supervision.

Funding: This work is supported by the Board of Research in Nuclear Sciences (BRNS- Grant No. 58/14/04/2021-BRNS/37092).

Conflicts of Interest: The authors have no conflicts to disclose.

Acknowledgments: Akanksha Gautam would like to acknowledge support from DST-INSPIRE (IF180930).

References

- Gabor D. A new microscopic principle. *nature*. 1948;161:777-8.
- Hendry D. *Digital Holography: Digital Hologram Recording, Numerical Reconstruction and Related Techniques*, U. Schnars, W. Jueptner (Eds.), Springer, Berlin (2005), ISBN: 354021934-X.
- Lee WH. Sampled Fourier transform hologram generated by computer. *Applied Optics*. 1970 Mar 1;9(3):639-43.
- Considine PS. Effects of coherence on imaging systems. *JOSA*. 1966 Aug 1;56(8):1001-9.

-
5. Mills JP, Thompson BJ. Effect of aberrations and apodization on the performance of coherent optical systems. II. Imaging. *JOSA A*. 1986 May 1;3(5):704-16. 1
 6. Rosen J, Brooker G. Digital spatially incoherent Fresnel holography. *Optics letters*. 2007 Apr 15;32(8):912-4. 2
 7. Vijayakumar A, Kashter Y, Kelner R, Rosen J. Coded aperture correlation holography—a new type of incoherent digital holograms. *Optics Express*. 2016 May 30;24(11):12430-41. 3
 8. Wu J, Zhang H, Zhang W, Jin G, Cao L, Barbastathis G. Single-shot lensless imaging with fresnel zone aperture and incoherent illumination. *Light: Science & Applications*. 2020 Apr 7;9(1):53. 4
 9. Naik DN, Ezawa T, Singh RK, Miyamoto Y, Takeda M. Coherence holography by achromatic 3-D field correlation of generic thermal light with an imaging Sagnac shearing interferometer. *Optics express*. 2012 Aug 27;20(18):19658-69. 5
 10. Naik DN, Pedrini G, Osten W. Recording of incoherent-object hologram as complex spatial coherence function using Sagnac radial shearing interferometer and a Pockels cell. *Optics Express*. 2013 Feb 25;21(4):3990-5. 6
 11. Roy M, Svahn P, Cherel L, Sheppard CJ. Geometric phase-shifting for low-coherence interference microscopy. *Optics and Lasers in Engineering*. 2002 Jun 1;37(6):631-41. 7
 12. Hariharan P, Oreb BF, Eiju T. Digital phase-shifting interferometry: a simple error-compensating phase calculation algorithm. *Applied optics*. 1987 Jul 1;26(13):2504-6. 8
- 9
- 10
- 11
- 12
- 13
- 14
- 15